Physica B 639 (2022) 413981

Contents lists available at ScienceDirect

Physica B: Physics of Condensed Matter

journal homepage: www.elsevier.com/locate/physb

Investigation of structural, electrical and photoresponse properties of composite based Al/NiO:CdO/p-Si/Al photodiodes

Ezgi Gürgenç [a,*], Aydın Dıkıcı [a], Fehmi Aslan [b]

[a] Energy Systems Engineering, Faculty of Technology, Firat University, Elazig, Turkey
[b] Rail Systems Machinery Technology, Yeşilyurt Vocational School, Turgut Özal University, Malatya, Turkey

ARTICLE INFO

Keywords:
Composite photodiode
Thin film
Nanomaterial
Photoresponse
Solar irradiation

ABSTRACT

In the present study, different molar ratios of (1:0, 0:1, 3:1, 1:1, and 1:3) NiO:CdO composite thin films were coated on p-Si by a dynamic sol-gel spin coating method. Structural characterizations of NiO:CdO thin films were performed by XRD, FE-SEM, and EDX analysis. The photoresponse and electrical behavior of the fabricated photodiodes were determined by current-voltage (I–V), transient photocurrent-time (I–t), capacitance-voltage (C–V), conductivity-voltage (G-V), and transient photocapacitance-time (C–t) measurements. All fabricated photodiodes were exhibited rectifying properties and the photocurrent values increased as the light intensity was increased. All photodiodes are sensitive to light and it was determined that the NiO photodiode exhibited the highest photosensitivity value. Photocapacitance and photoconductance values of photodiodes were affected by light. Photoresponse and electrical behavior were affected by the interface states and the NiO:CdO ratio. The results show that Al/NiO:CdO/p-Si/Al photodiodes can be used as photosensors or photocapacitors in opto-electronic applications.

1. Introduction

The development of green energy technology has become a very urgent issue in recent years because of intense changes in the global climate [1]. One of the most important renewable energy sources is solar energy. The conversion of solar energy to electricity is carried out by both flat photovoltaic (PV) and concentrated solar power (CSP) systems. The low energy production efficiency of solar energy conversion systems is often criticized by public [1–3]. One of the most effective methods to increase the harvesting time of solar energy is to use solar panel tracking systems [1,2]. With this system, they are oriented at optimum tilt angles from the horizon to the equator to maximize the solar radiation on the solar panels. In addition, the panels are placed in an optimum position vertically to the sun's rays during the day. In this way, energy conversion efficiencies are increased by making more use of sunlight [4,5]. In order to increase the energy production efficiency of solar collectors and panels, one of the sensors that is frequently used for direct detection of light in solar panel tracking systems and in the electronics industry are photodiodes that are sensitive to light [6,7]. Photodiodes are circuit elements that accept an optical signal and convert it into an electrical output [8,9]. With the developing technology, metal oxide semiconductor based Schottky, p-i-n, p-n, and heterojunction photodiodes have become promising devices for electro-optical communication and optoelectronic systems [7,10].

The metal-semiconductor structures, transistors, radio frequency detectors, photodiodes and solar cells have been formed an important part of semiconductor devices for many years [11]. Silicon (Si) and metal oxide semiconductor materials are the most promising materials in electronic device production, and these materials are used to produce new types of photodiodes due to their interesting electronic behavior [10]. Semiconductor metal oxides such as titanium dioxide (TiO_2), zinc oxide (ZnO), cadmium oxide (CdO), tin oxide (SnO_2), and nickel oxide (NiO) are frequently used in photodiodes. The NiO, one of these metal oxide semiconductors is quite interesting, due to has wide band gap (3.6–4.0 eV), p-type conductivity, large exciton binding energy, high hole mobility, low material cost, promising ion storage, optical properties and can be fabricated by different methods. Because of these interesting properties, NiO are effectively used in lithium-ion batteries, solar cells, supercapacitors, chemical sensors, photodiodes, and electrochromic coatings. In addition, CdO is preferred in photovoltaic solar cells, optoelectronic devices, liquid crystal displays, solar cells, lasers, and photodiodes due to its band gap (2.15 eV–2.7 eV) with low electrical

* Corresponding author. Energy Systems Engineering, Faculty of Technology, Firat University, 23119, Elazig, Turkey.
E-mail address: ezgigurgenc89@gmail.com (E. Gürgenç).

https://doi.org/10.1016/j.physb.2022.413981
Received 23 February 2022; Received in revised form 31 March 2022; Accepted 29 April 2022
Available online 1 May 2022

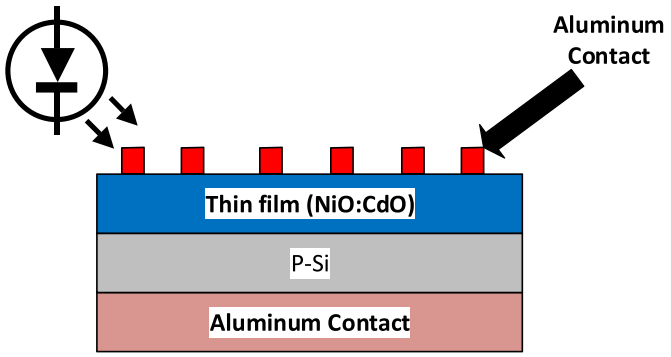

Fig. 1. The representative image of fabricated Al/NiO:CdO/p-Si/Al photodiode.

resistance, high carrier concentration, cadmium interspaces, natural defects of oxygen vacancies, low resistance, and sensitivity in the near ultraviolet region and high transparency [9,12–16]. The Si is also a very suitable material for visible and UV photodetection applications due to its narrow band gap of 1.1 eV [9]. The photoresponse and electrical properties of Si and metal oxide-based photodiodes can be improved by using a second metal oxide. This is because the second metal oxide changes the electrical and optical properties of the active layer used in the photodiode production [10]. For this reason, composite photodiodes can largely meet the expectations of benefiting from clean solar energy [17]. The Si and metal oxide-based photodiodes can be fabricated using different thin-film coating methods such as DC and RF sputtering, pulsed laser deposition, electrochemical deposition, chemical vapor deposition, sol-gel, and spray pyrolysis. Although all these techniques have their own advantages and disadvantages, sol-gel coating method has much great attention due to the low temperature production, low cost, wide area coating, low precursor volume, high purity, homogeneity, non-vacuum technique, and easy technology [9,17–20].

Many studies about the fabrication of photodiodes by pure CdO, pure NiO and doping different elements to these metal oxides on p-Si, n-Si and ITO glass are available in the literature to investigate their photoresponse and electrical properties [7], [9,18,21–24]. Moreover, ZnO:TiO_2 [25], CdO:TiO_2 [26], ZnO:CdO [8,27], ZnO:NiO [28], and ZnO:MgO [10], composite based photodiodes were produced by different researchers and electrical, and photoresponse properties were investigated. Photodiodes consisting of p-n heterojunction thin films have become one of the promising alternatives for optoelectronic applications in recent years and there is a little knowledge about NiO:CdO photodiodes from these p-n structures [29]. As mentioned above, the studies have mainly examined the doped and un-doped NiO, and CdO photodiodes with different elements. However, the researches on the fabrication and characterization of photodiodes by combining different metal oxide semiconductors in a composite film are still limited. Therefore, photodiodes based on different metal oxide semiconductor composites are considered to be a topic that needs to be investigated currently. In addition, in our knowledge, it was seen that there were no study related to photodiodes consisting of NiO:CdO composite structures, which is one of the p-n type structures. For this purpose, in the present study, it is aimed to fabricated the Al/NiO:CdO/p-Si/Al composite photodiodes by a dynamic sol-gel spin coating method, characterized and determined the photosensitivity, and electrical properties of which have not been investigated in the literature to the best of our knowledge.

In this study, Al/NiO:CdO/p-Si/Al photodiodes were fabricated by a dynamic sol-gel spin coating method. Structural properties of thin films were analyzed by X-ray diffraction (XRD), field emission scanning electron microscopy (FE-SEM), and energy dispersive X-ray spectroscopy (EDX). The electrical and photoresponse properties of the fabricated composite-based photodiodes were performed using the KEITHLEY 4200 semiconductor characterization system and the FYTRONIX 7000 solar simulator.

2. Material and methods

In the present study, pure NiO, pure CdO, and different molar ratios of NiO:CdO composite thin films were deposited on p-Si layer by dynamique sol-gel spin coating technique. The Chemsolute brand 2-methoxyethanol ($CH_3OCH_2CH_2OH$) was used as the solvent and Chemsolute brand monoethanolamine ($NH_2CH_2CH_2OH$) was used as the stabilizer. Acros Organics brand Cadmium acetate dehydrate ($C_4H_6CdO_4{\cdot}2H_2O$) was used as Cd source and Carlo Erba brand Nickel (II) acetate tetrahydrate ($Ni(OCOCH_3)_2{\cdot}4H_2O$) was used as Ni source for preparing sol-gel solutions. The 0.5 M of Ni and Cd in molar ratios of Ni:Cd (1:0, 0:1, 3:1, 1:1, and 1:3) were poured into 10 ml solvent and mixed on a magnetic stirrer as long as all the powders were dissolved. The 0.5 M of stabilizer was dropwise to the mixture while the stirring was continued at 80 °C for 2 h and thereafter the sol-gels required for the coatings were prepared. The p-Si sheet (⟨100⟩ orientation, the thickness of 600 μm and the resistance of 1–10 cm-Ω) was consecutively cleaned with acetone, distilled water, ethanol, and distilled water for 5 min each in ultrasonic bath. Then, this plate was immersed in 1:10 HF:H_2O solution for 30 s and ultrasonically washed in distilled water for 5 min. For ohmic contacts, the opaque side of the p-Si layer was coated with 99.99% pure Aluminum (Al) at a thickness of 150 nm. This coating process was carried out in Nanovak brand vacuum thermal evaporation device and after this coating process, the p-Si layer was annealed under nitrogen gas at 570 °C for 5 min, and finally cut in pieces. Sol-gel solutions, which were left to rest for 24 h at room temperature, were deposited on p-Si sheets at 3000 rpm for 30 s with a dynamic spin coating technique by using Fytronix brand spin coater device and dried at 150 °C for 10 s. The dried samples were kept at room temperature for 10 min and the same procedures were repeated, hence two-layer coating was performed. The coated samples were calcined in the oven at 450 °C for 1 h. The top of thin films was coated with 99.99% pure Al using a Nanovak brand vacuum thermal evaporator with a physical mask and upper contacts were obtained. Thus, Al/NiO:CdO/p-Si/Al composite based photodiodes with different molar ratios were fabricated. The structural properties of the fabricated photodiodes were investigated with the PANalytical Empyrean brand X-ray diffraction (XRD) device. The XRD analyses were performed in CuKα (λ = 1.5406 °A) radiation at 2θ = 20–80° scanning range, 0.0262606° scanning step and 45 kV/40 mA. The surface morphologies and chemical compositions of the photodiodes were analyzed by Zeiss Crossbeam 540 brand field emission scanning electron microscopy (FE-SEM) and energy dispersive X-ray spectroscopy (EDX), respectively. The photoresponse and electrical measurements were carried out by KEITHLEY 4200 brand semiconductor characterization system and FYTRONIX 9000 brand solar simulator. Fig. 1 shows the representative image of the fabricated photodiode.

3. Results and discussion

3.1. Structural and morphological characterization of NiO:CdO thin films

Fig. 2 shows the XRD patterns of fabricated pure NiO, pure CdO and composite NiO:CdO nanostructures. The pure NiO and CdO peaks are match well with JCPDS card no. 47–1049 and JCPDS card no. 75–0594, respectively. According to these cards, both NiO [15,30,31] and CdO [32,33] are cubic-structured. The 2θ angles of diffraction planes are given in Table 1. The intense peaks observed in NiO thin film coating at 2θ angles of 37.26°, 43.30°, 62.92°, 75.48°, 79.44°, and observed in CdO thin film coating at 2θ angles of 33.01°, 38.29°, 55.28°, 65.91°, and 69.25° corresponding to (111), (200), (220), (311), and (222) planes, respectively. The high intensities of the (111) and (200) planes indicate that NiO is crystalline. The absence of secondary phases and impurities in the XRD diffraction peaks verify that NiO and CdO have been

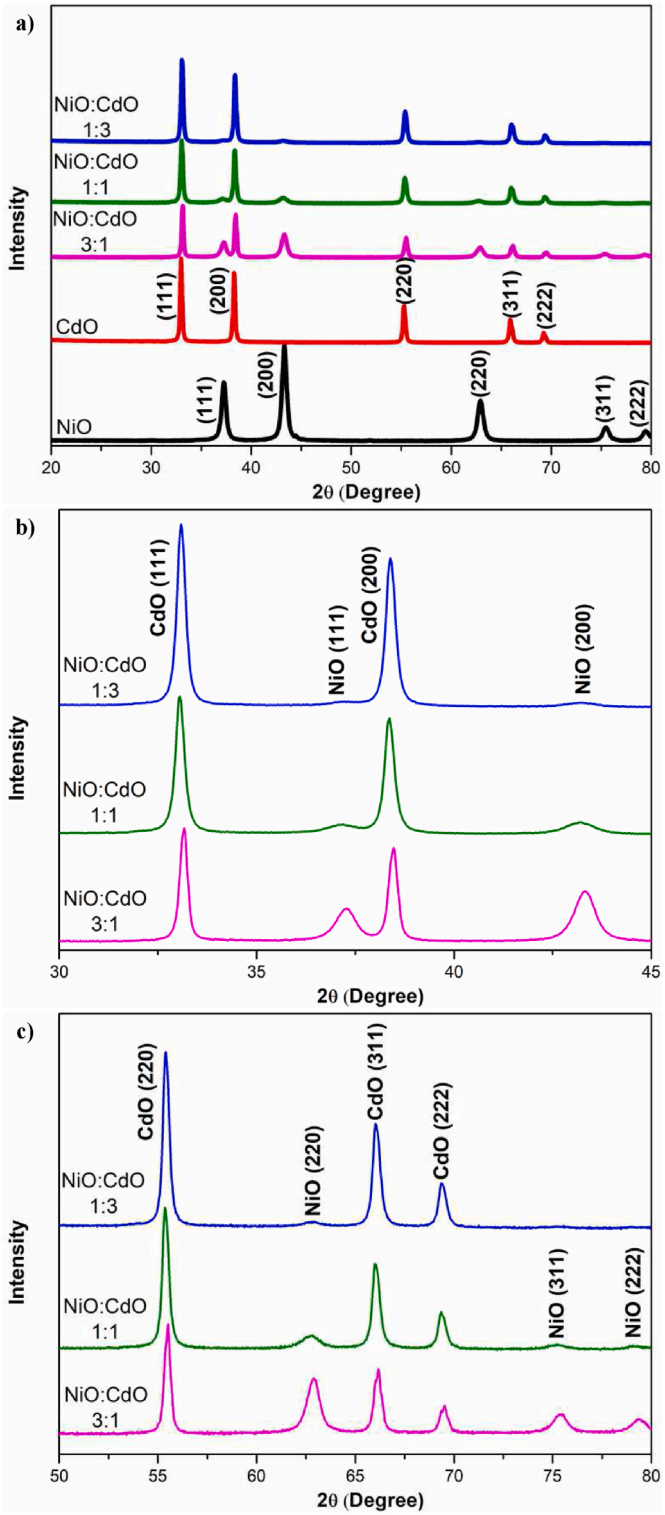

Fig. 2. XRD results of fabricated NiO:CdO thin film coatings at different 2θ scanning ranges. a) 20–80°, b) 30–45°, and c) 50–80°.

successfully formed with high purity [15,30–34]. The high intensity of the (111) plane in CdO refers the polycrystalline nature [35,36]. The peak positions and intensities of the composite thin films are different from those of pure NiO and pure CdO. Nonetheless, they are perfectly matched with JCPDS card no. 47–1049 and JCPDS card no. 75–0594, respectively. In addition, characteristic diffraction peaks of both NiO and CdO were observed in composite thin films and the intensities of characteristic peaks increased with increasing NiO or CdO ratio in composite thin films. Also no different phases or impurities were determined in composite thin films. Consequently, the results confirm that the NiO:CdO composite thin films were successfully fabricated and the composites are cubic-structured with high purity [37,38].

Table 1
The 2θ angles of diffraction planes.

Photodiode	Oxide	111	200	220	311	222
NiO	NiO	37.26°	43.30°	62.92°	75.48°	79.44°
CdO	CdO	33.01°	38.29°	55.28°	65.91°	69.25°
NiO:CdO (3:1)	CdO	33.16°	38.45°	55.49°	66.17°	69.54°
	NiO	37.29°	43.33°	62.89°	75.42°	79.38°
NiO:CdO (1:1)	CdO	33.06°	38.36°	55.35°	66.02°	69.35°
	NiO	37.18°	43.20°	62.76°	75.18°	79.17°
NiO:CdO (1:3)	CdO	33.09°	38.39°	55.41°	66.04°	69.38°
	NiO	37.23°	43.22°	62.81°	-	-

Fig. 3 shows the FE-SEM images and the EDX results of NiO:CdO composite thin films coated on p-Si layers. All films were successfully formed on p-Si layers and crack-free, and homogeneous coating layers were obtained. Thin film coatings are composed of nanostructures. While it is composed of fine-grained aggregated nanoparticles in NiO coating, nano flower-like structures are encountered in CdO coating. Similar findings are reported in previous studies [39–43]. On the other hand, composite coatings have different structure when compared to these two coatings and are composed of quasi-spherical, non-uniform, and stacked granule-like (white areas) structures similar to the literature study [44]. The density of these structures in the coating decreased by increasing the NiO ratio in the composite structure. Except for the composite photodiode with a NiO:CdO ratio of 1:1, the noise did not occur in the EDX analyzes of the other samples. In EDX analysis, the K_α, K_β and K_γ lines in the K shell accelerate the emissions. The probabilities of each transition are different, causing the individual lines measured in this case to be of different intensities [45]. According to the EDX analysis results, no different elements were found in NiO and CdO thin films, except for Si and O. The EDX results confirms with the XRD analysis. In composite thin films, the Ni:Cd ratios are 2.97, 0.85 and 0.34, respectively which are very close to the doping ratios. These results combining with the XRD results, the composite structures have been successfully formed on p-Si layers.

3.2. The I–V characterization of fabricated photodiodes

Fig. 4 shows the I–V properties of the fabricated composite based photodiodes in the dark and at different light intensities (20–100 mW/cm^2). As can be seen in Fig. 4, the I–V properties of fabricated photodiodes varied with the NiO:CdO ratio. Quite pronounced differences were observed in the negative bias region between dark and illumination and under illumination, the reverse current values of Al/NiO:CdO/p-Si/Al photodiodes at any applied voltage are higher than that of under dark [14,46]. The forward current in the fabricated photodiodes tends to increase depending on the applied voltage and the reverse current distortions confirm that the diodes have rectifying properties [47]. As seen from the I–V graphs, all photodiodes are light sensitive. The change in reverse current with applied voltage can be associated with photon excitation of charge carriers from the valence band to the conduction band. Since the light coming to the photodiodes creates electron-hole pairs, the current increases as the light intensity increases at the reverse bias voltage, while it remains almost constant at the forward bias voltage. It is related that free charge carriers can contribute to the current [14,47–49]. The increase in current with increasing illumination intensity in the reverse bias region supports the photovoltaic properties of the fabricated photodiodes [46]. The rectification ratio (RR) graphs of the fabricated photodiodes in the dark and at different light intensities, which is the ratio of forward current (I_F) at (+5 V) to reverse current (I_R) at (−5 V) (I_F/I_R), are shown in Fig. 5. The RR values of the photodiodes

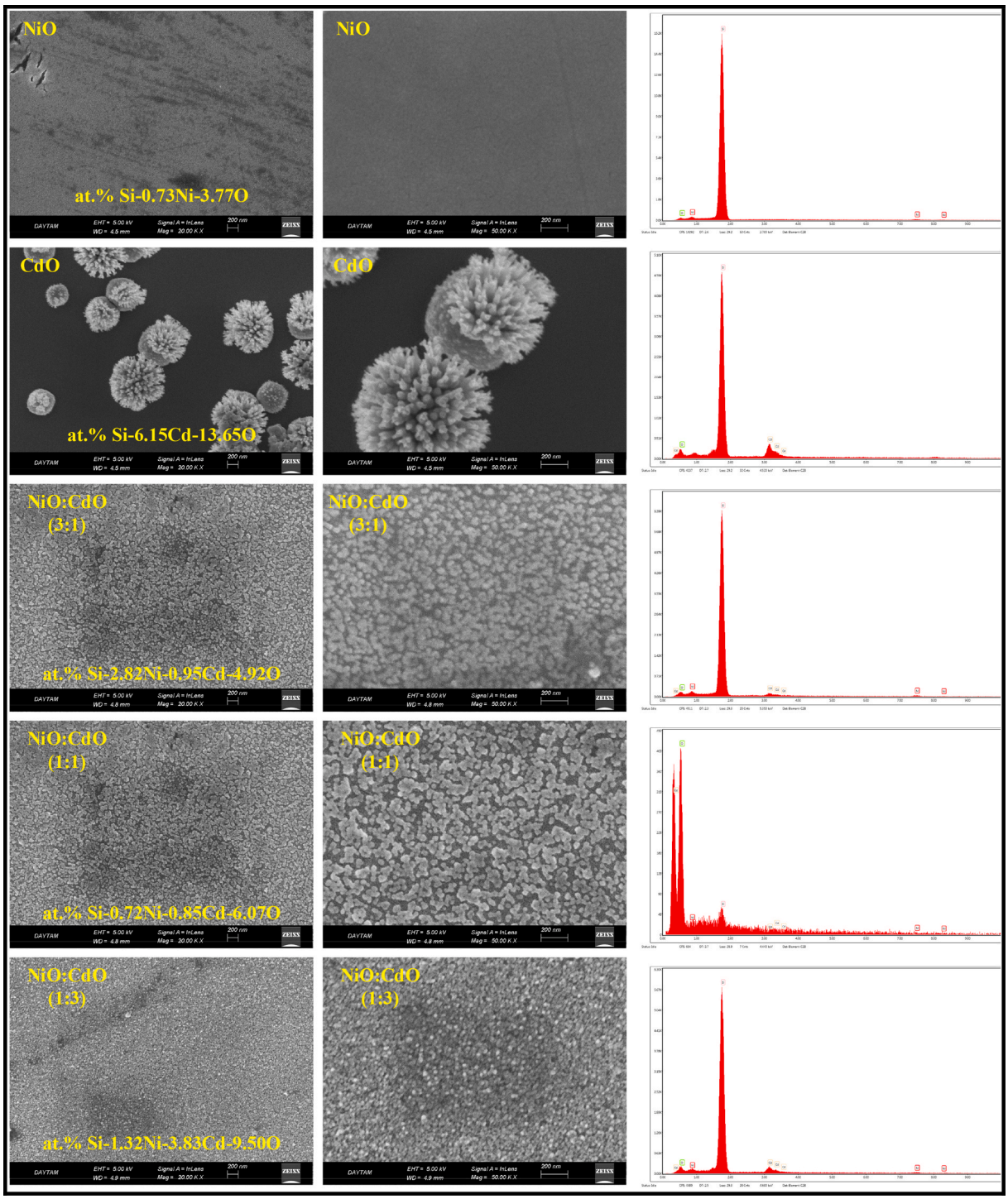

Fig. 3. FE-SEM images and EDX results of fabricated NiO:CdO thin films.

in the dark state are 1.60×10^4, 5.76×10^2, 8.14×10^3, 6.24×10^3 and 2.23×10^3 for 1:0, 0:1, 3:1, 1:1, and 1:3 respectively according to the NiO:CdO ratio. These values showed a decrease when the light was turned on and decreased as the light intensity increased. This shows the passage of the electrons from the valence band to the conduction band due to light absorption [47]. The RR values of composite photodiodes under light are higher than those of pure photodiodes. As the CdO ratio in the composite film enhanced, the RR value decreased. These results show that the fabricated photodiodes exhibit photoconductive behavior.

To investigate the influence of the NiO:CdO ratio on the diode properties in the fabricated photodiodes, it is necessary to find parameters such as barrier height (φ_b) and ideality factor (n), which have a vital place in photodiodes. The φ_b and n values of the photodiodes can be calculated using the Thermionic Emission Theory (TET) expressed by the equation below [9,13,50];

$$I = I_0\left(\exp\left(\frac{qV - IR_s}{nkT}\right)\right) - 1 \quad (1)$$

where I_0, V, T, k, q and R_s denote saturation current, applied voltage, absolute temperature, Boltzmann constant, electron charge and series resistance, respectively. The term I_0 can be calculated using the following relationship [9,49];

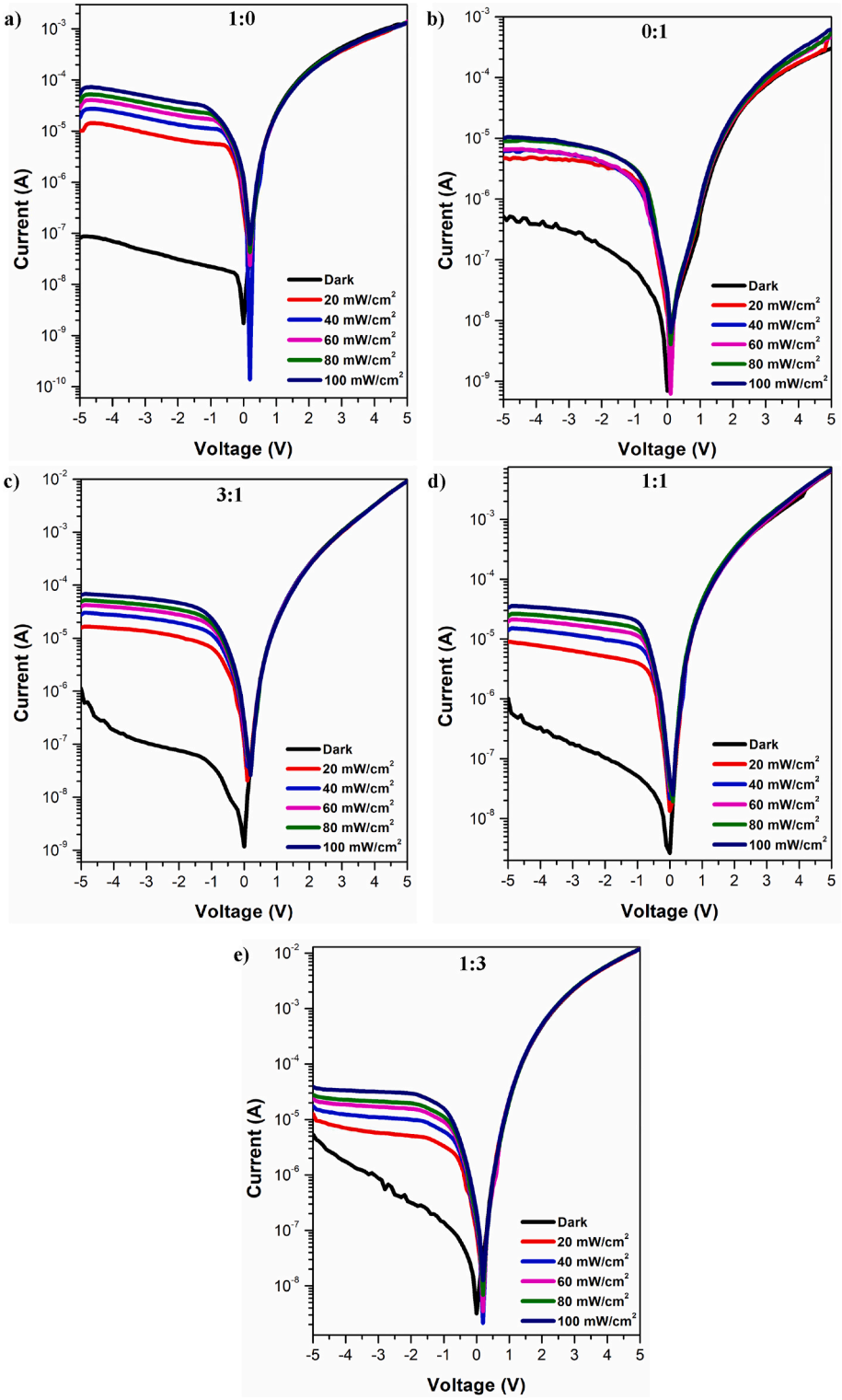

Fig. 4. I–V characteristics of fabricated photodiodes at different NiO:CdO ratios a) 1:0, b) 0:1,c) 3:1, d) 1:1, and e) 1:3.

$$I_0 = AA^* T^2 \exp\left(-\frac{q\varphi_b}{kT}\right) \quad (2)$$

where A* is Richardson's constant and its value for p-Si is 32 A/cm^{2}K^2. A is the calculated diode area and its value is 7.85 × 10^3 cm^2. The intersection and slope of the forward bias current versus the I–V plot are used to find the values of φ_b and n, respectively. Equation (1) and Equation (2) can be rearranged to find these values using the following equations [9];

$$n = \frac{q}{kT}\left(\frac{dV}{d(lnI)}\right) \quad (3)$$

$$\varphi_b = \frac{kT}{q} ln\left(\frac{AA^* T^2}{I_0}\right) \quad (4)$$

The calculated n and φ_b values are given in Table 2. As the change in NiO:CdO ratio, there were variations in those values. In fabricated

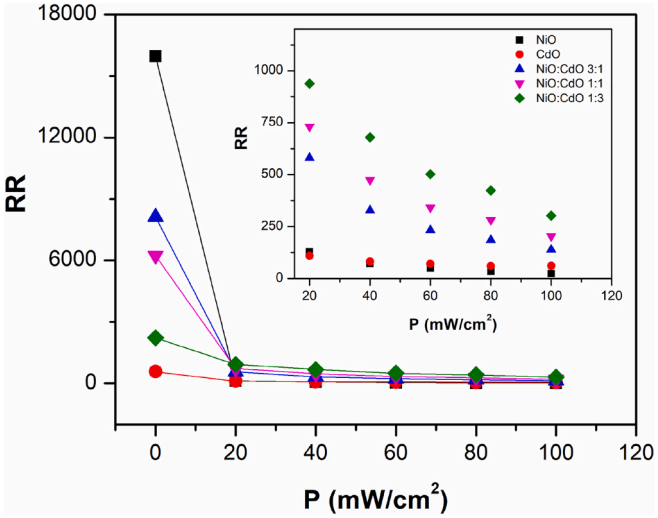

Fig. 5. The RR values of the fabricated photodiodes according to the light intensity.

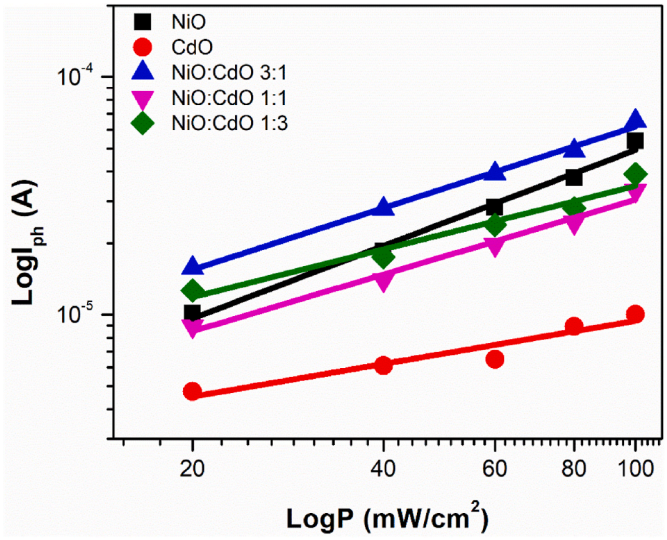

Fig. 7. Plots of I_{ph} - P of fabricated photodiodes.

Table 2
The n and φ_b values of the fabricated photodiodes.

Fabricated photodiode	n	φ_b (eV)
NiO	6.85	0.4178
CdO	4.01	0.4356
NiO:CdO (3:1)	7.05	0.4179
NiO:CdO (1:1)	6.03	0.4128
NiO:CdO (1:3)	8.17	0.4169

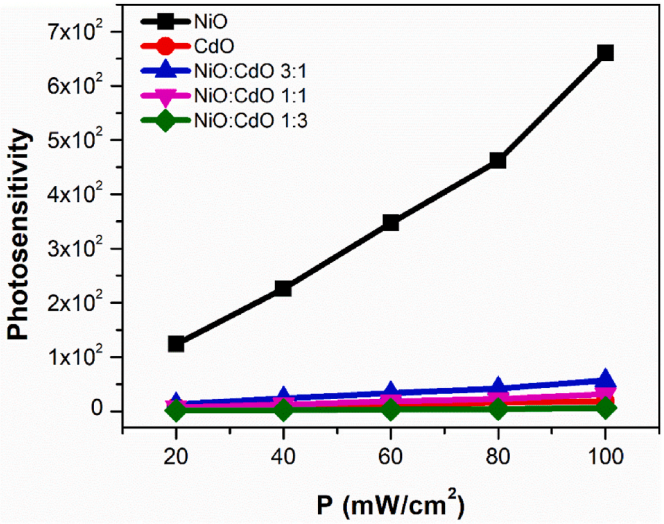

Fig. 6. The PS values of the fabricated photodiodes according to the light intensity.

photodiodes, the n value, which should be one for an ideal diode, are 6.85, 4.01, 7.05, 6.03 and 8.17 for 1:0, 0:1, 3:1, 1:1, and 1:3, respectively according to the NiO:CdO ratio. The n value also changed at different ratio of NiO:CdO and as seen from the results, it differs from the value that an ideal photodiode should have. This can be related to the interface film layer, series resistance, interface states, tunneling effect and inhomogeneous barrier [9,51,52]. The barrier heights were also slightly affected by NiO:CdO ratio, and the lowest φ_b value was obtained in the composite photodiode with a 1:1 NiO:CdO ratio. These results show that the fabricated Al/NiO:CdO/p-Si/Al photodiodes have

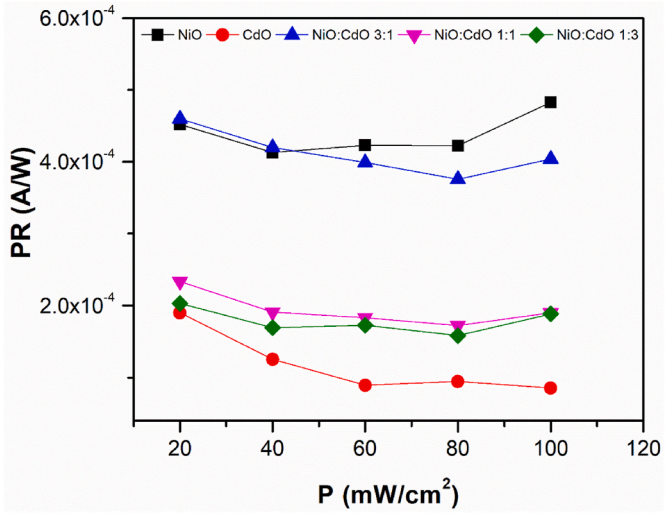

Fig. 8. The PR values of the fabricated photodiodes according to the light intensity.

nonlinear behavior [14].

The photosensitivity (PS) of the photodiodes was calculated at -5 V using Equation (5) [7] and these values are shown in Fig. 6.

$$PS = \frac{I_{ph} - I_{dark}}{I_{dark}} \quad (5)$$

Here, I_{ph} and I_{dark} are photocurrent and dark current, respectively. All photodiodes have a higher reverse current value under illumination than that of in the dark, and the photodiode with the highest light sensitivity is NiO photodiode. As reported in literature study, that the PS value of the pure photodiode is higher than those of Zn-doped NiO photodiodes [47]. The photosensitivity of the photodiodes increased as the light intensity increased, and as the NiO:CdO ratio changed, photodiodes with different light sensitivity emerged. Similar results were obtained in a similar study in the literature [47]. With the addition of CdO to NiO, the work function of NiO has changed and caused a variation in the width of the depletion region of the diode. It is thought that this situation reduces the charge separation at negative voltages, causing composite photodiodes to show lower photosensitivity compared to NiO. In some optical communication applications, high photoresponse is desired, while in some applications, low photoresponse of controllers

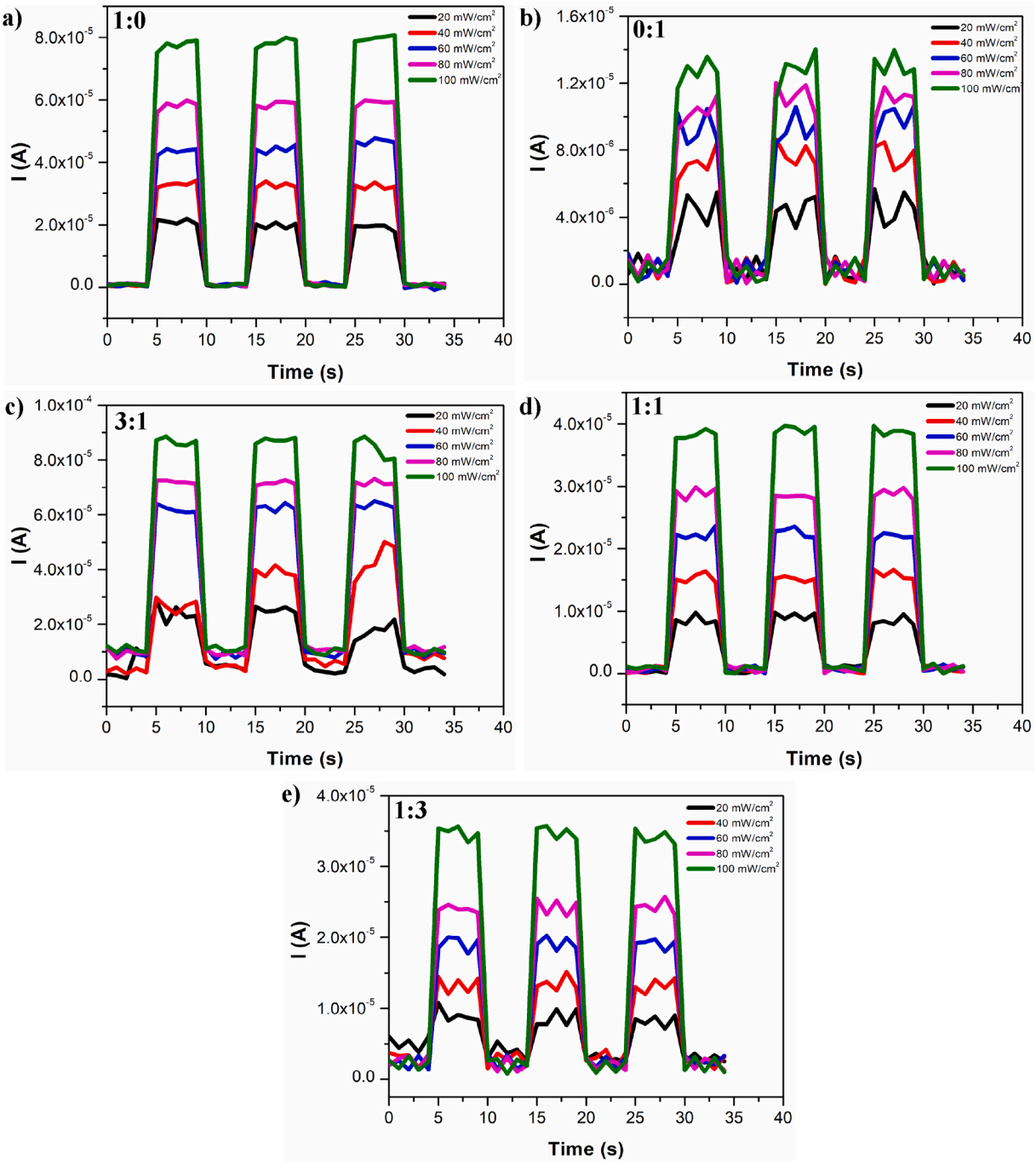

Fig. 9. Plots of transient photocurrent - time of fabricated photodiodes at different NiO:CdO ratios a) 1:0, b) 0:1, c) 3:1, d) 1:1, and e) 1:3.

may be required to switch a component of electronic devices [10]. It has been observed that the photoresponse can be controlled by changing the NiO:CdO ratio in photodiodes, and the fabricated photodiodes exhibited photoconductive behavior.

To better analysis the photosensitivity of the photodiodes, the illumination current was plotted against the illumination intensity and the results were plotted in log(I_{ph}) – log(P) graph (Fig. 7). The relationship between I_{ph} and light intensity (P) is expressed by the following equation [9];

$$I_{ph} = \alpha P^{m} \tag{6}$$

where, α is a constant and m is a coefficient. The m values can be find by using slope of the log(I_{ph})– log(P) plot. The m values of fabricated photodiodes according to NiO:CdO ratio are 1.014 (for 1:0), 0.456 (for 0:1), 0.861 (for 3:1), 0.793 (for 1:1), and 0.669 (for 1: 3). Also a study carried out by Pehlivanoğlu, the m value was found to be greater than 1 for pure NiO (1.12) [47]. In another study on NiO photodiodes, the m value was calculated as 1.29 [14]. The m value decreased as the CdO ratio increased in composite photodiodes. A similar situation was observed for ZnO:CdO composite photodiodes and the m value was 0.56 at high CdO ratio [27]. The recombination mechanism is explained by the value of m. When m is equal to 1 and 0.5, it refers to monomolecular and bimolecular, respectively. Additionally, in the range of 0.5 and 1 indicate that a continuous distribution of trap levels in regional situations [7,18,48]. Monomolecular recombination refers to an electron and hole recombination through the trap state or recombination center. Bimolecular recombination means that the density of carriers reaching

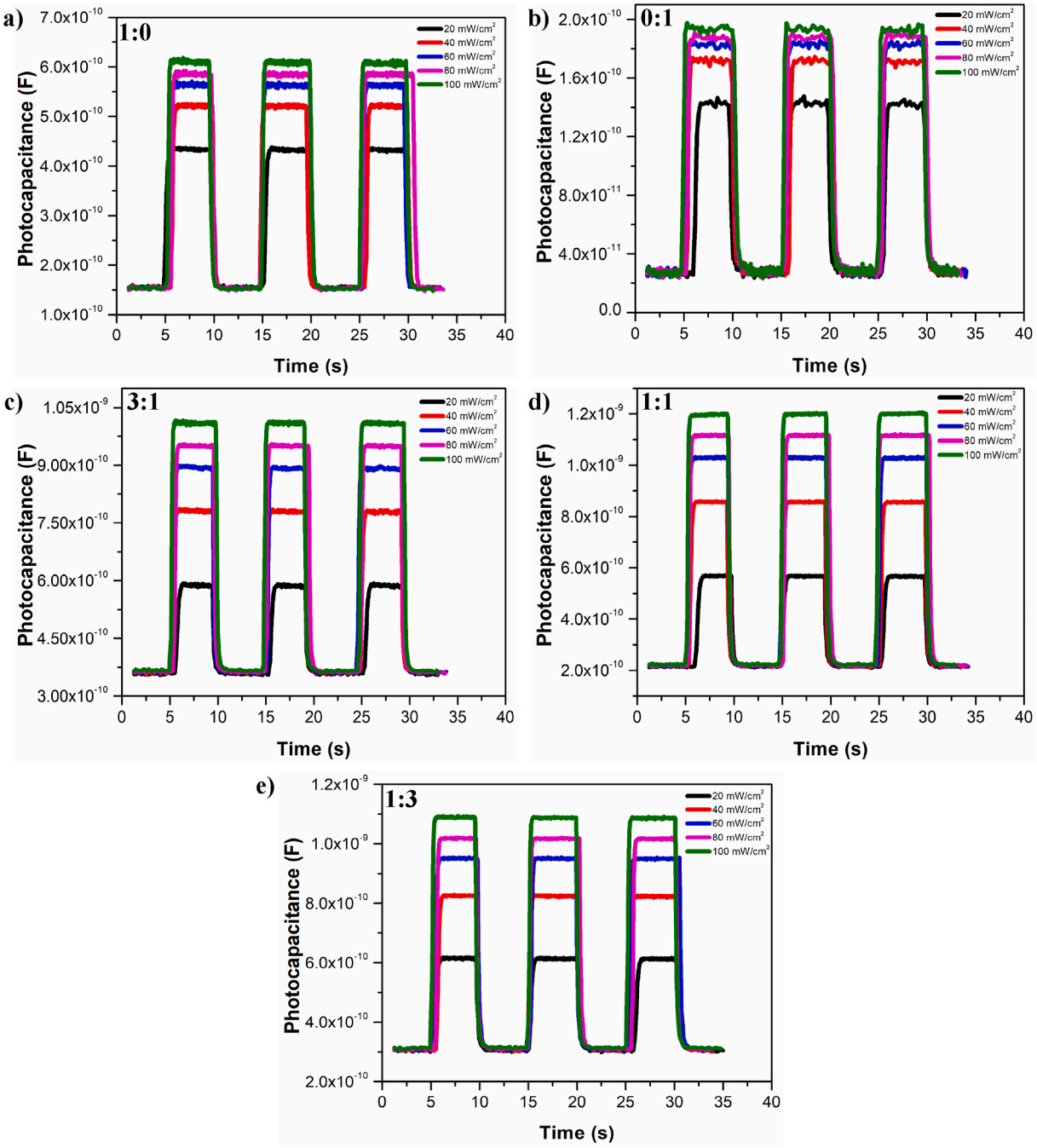

Fig. 10. Plots of transient photocapacitance - time of fabricated photodiodes at different. NiO:CdO ratios a) 1:0, b) 0:1, c) 3:1, d) 1:1, and e) 1:3.

the Fermi level is higher than that of below the Fermi level [47]. The m values obtained in this study show that the photoconductivity behavior of the fabricated photodiodes is linear. The recombination mechanisms of NiO and CdO photodiodes are monomolecular and bimolecular, respectively. Since the m values of composite photodiodes are between 0.5 and 1, the photoconductive mechanisms of these photodiodes can be controlled by the presence of a continuous distribution of trap levels [14]. The photoresponsivity (PR) values of the fabricated photodiodes can be calculated using Equation (7) given below [47];

$$PR = \frac{I_{ph} - I_{dark}}{PA} \tag{7}$$

Here, A is the surface area of the photodiode. As shown in Fig. 8, The PR values of the fabricated photodiodes affected by light intensity. Photodiodes are sensitive at all light intensities and the PR values at 100 mW/cm^2 light intensity are 4.83×10^{-4} A/W, 8.54×10^{-5} A/W, 4.04×10^{-4} A/W, 1.90×10^{-4} A/W and 1.88×10^{-4} A/W for 1:0, 0:1, 3:1, 1:1, and 1:3, respectively according to the NiO:CdO ratio. In the study performed by Gozeh et al. the PR value for pure CdO was found as 1×10^{-5} A/W [9]. The photodiode with the highest PR value at light intensities of 60–100 mW/cm^2 is NiO and the photodiode with the lowest PR value at all light intensities is CdO. At 20 mW/cm^2 and 40 mW/cm^2 of light intensities, NiO:CdO ratio of 3:1 provided the highest PR value in composite photodiode. Also at all composite photodiodes as the CdO ratio increased the PR values decreased. All photodiodes are light sensitive and their PR values were change as the NiO:CdO ratio changes.

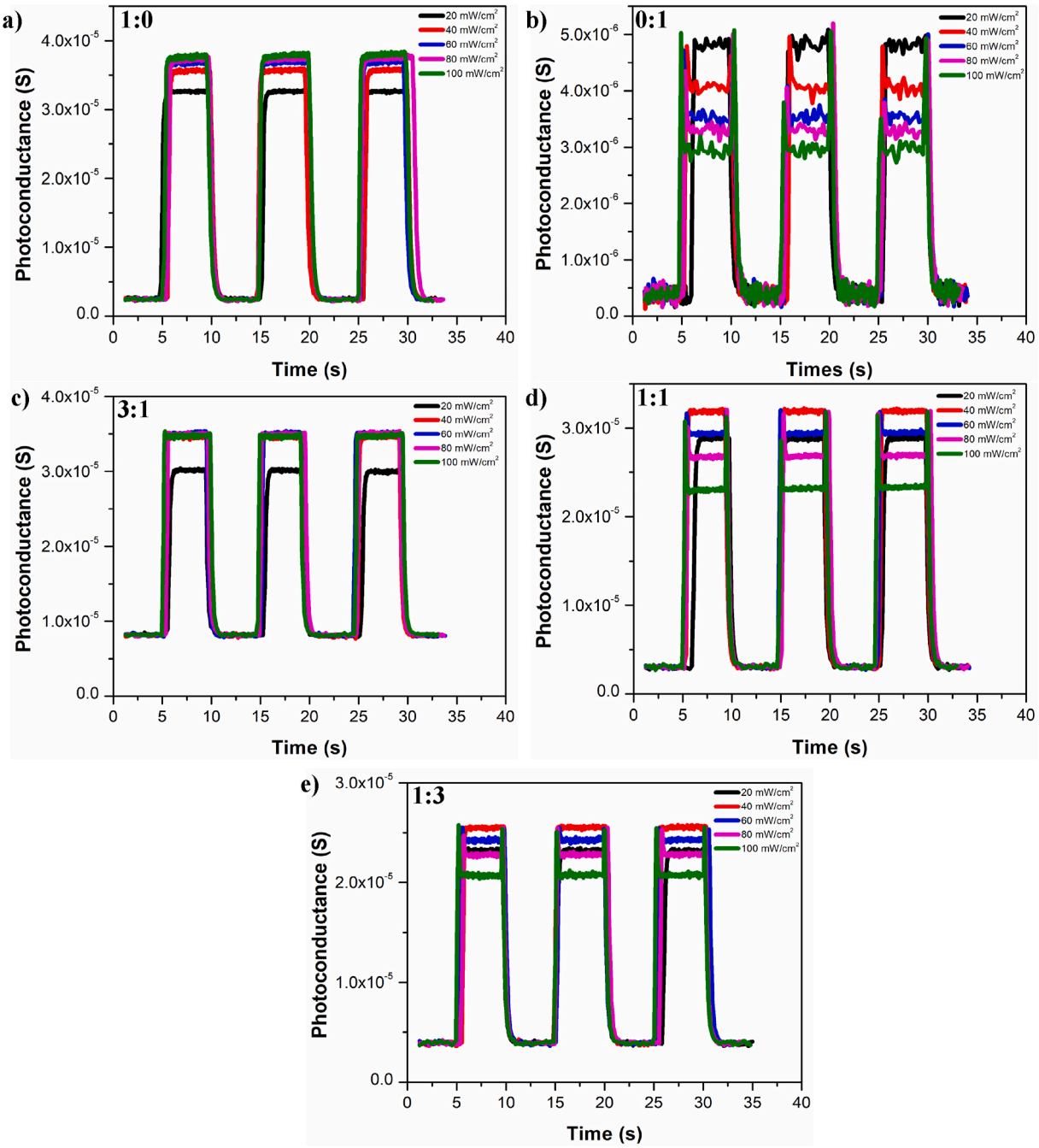

Fig. 11. Plots of photoconductance - time of fabricated photodiodes at different NiO:CdO ratios a) 1:0, b) 0:1, c) 3:1, d) 1:1, and e) 1:3.

3.3. I–t and C–t characteristics of fabricated photodiodes

Photocurrent-time characterizations play a key role in better understanding the photoconductivity mechanisms of photodiodes. The transient photocurrent measurement results of the fabricated photodiodes at -5 V and different illumination intensities (20–100 mW/cm^2) are shown in Fig. 9. Sudden increases were observed in photocurrents as the light intensity was increased, this was due to the fact that photodiodes created more charge carriers with solar radiation in the depletion region. The increase in photocurrents with increasing light intensity indicates that the fabricated photodiodes have good photoconductive behavior [51,53]. With illumination, photocurrents rise up to the saturation level, this is because free charge carriers are formed and their number increases and photogenerated electrons contribute to the current [14,47,51]. When the illumination was terminated, the photocurrents rapidly decreased to the initial level due to the trapped charge carriers at deep levels [14,18,47]. As the lighting was turned on and off, the above-mentioned behavior repeated. These repetitions indicate that the fabricated photodiodes show reversible switching behavior [47]. The photocurrent values of the fabricated photodiodes under 100 mW/cm^2 light intensity are 7.90 × 10^{-5}, 1.36 × 10^{-5} A, 8.85 × 10^{-5} A, 3.92 × 10^{-5} A and 3.56 × 10^{-5} A for 1:0, 0:1, 3:1, 1:1, and 1:3, respectively according to the NiO:CdO ratio. The photocurrent values of pure NiO and pure CdO photodiodes in this study are in agreement with the values of NiO and CdO photodiodes in previous studies [7,14,15,18]. The highest photocurrent value was obtained in the composite photodiode with the lowest CdO ratio, and the increase in the CdO ratio led to the photocurrent values to decrease. This decrease in the photocurrent is thought to be due to the high CdO presence increasing the NiO carrier concentration. The increase of this carrier concentration may decrease

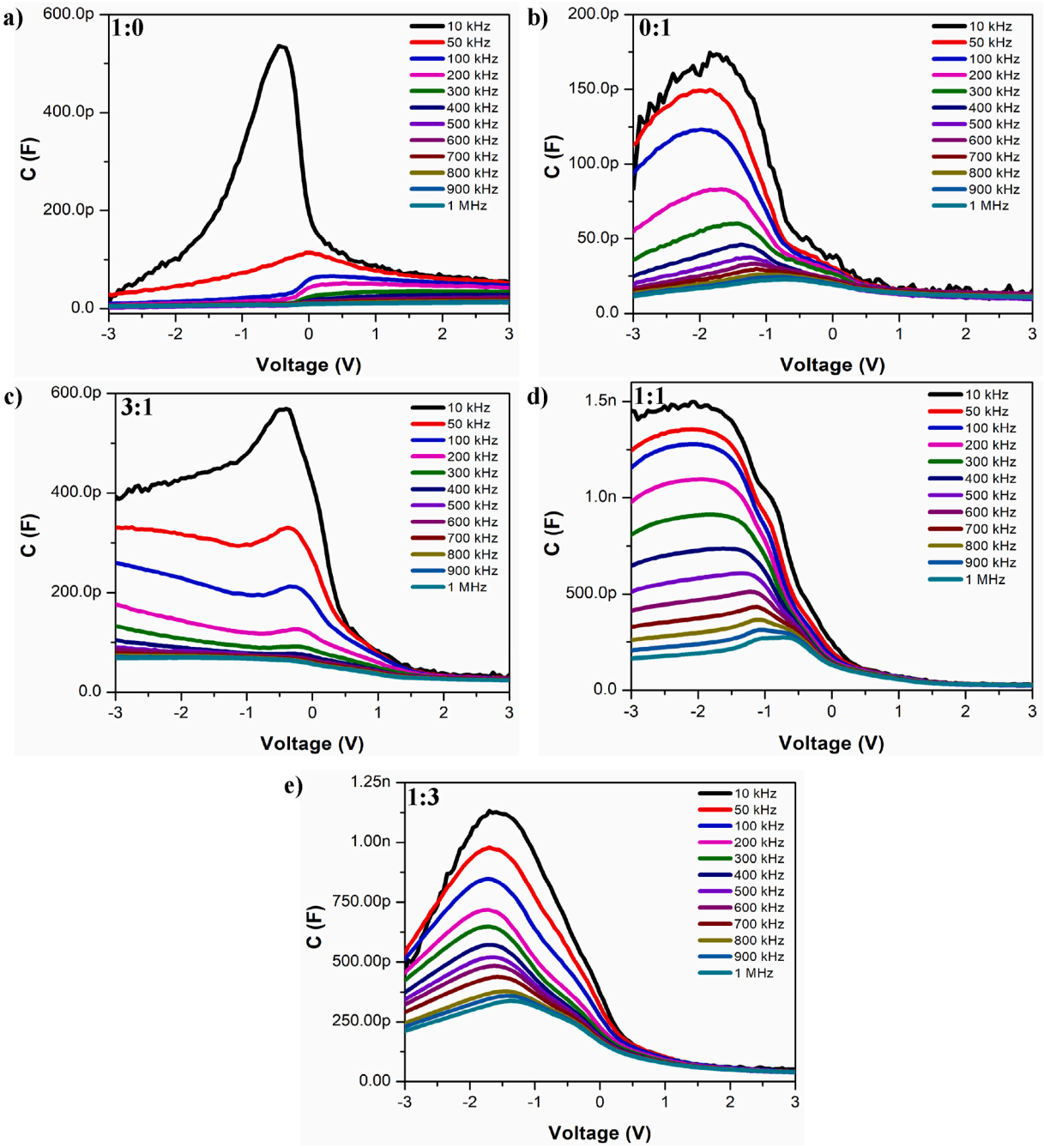

Fig. 12. The C–V characteristics of fabricated photodiodes at different NiO:CdO ratios a) 1:0, b) 0:1, c) 3:1, d) 1:1, and e) 1:3.

the carrier mobility by disrupting the surface electric field, and this may increase the photoresponse times [47]. The photoresponse properties of photodiodes can be changed and controlled by the NiO:CdO ratio.

The time-dependent changes of photocapacitance and photoconductance of the fabricated photodiodes at 10 kHz and different light intensities (20–100 mW/cm^2) are shown in Fig. 10 and Fig. 11, respectively. The photocapacitance and photoconductance of all fabricated photodiodes were affected by the light intensity. When the light was turned on, the photocapacitance suddenly increased and became saturated. As long as the light was applied, it remained stable and when the light was turned off, the photocapacitance returned to its previous level without any deterioration. As the light intensity was increased, the photocapacitance also improved. This may due to the higher production of free charge carriers under light [14,51]. The photocapacitance values of the photodiodes under 100 mW/cm^2 light intensity are 0.62 nF, 0.2 nF, 1.02 nF, 1.19 nF and 1.09 nF for 1:0, 0:1, 3:1, 1:1, and 1:3, respectively according to the NiO:CdO ratio. The highest photocapacitance value was reached in the composite photodiode containing half on half NiO and CdO, and the photocapacitance values of the composite photodiodes were higher than the pure ones. The photoconductance values suddenly increased when the light was turned on and returned to its former value after reaching a certain saturation value. Sudden changes in photocapacitance and photoconductance values due to illumination confirm that the fabricated photodiodes exhibit photocapacitive and photoconductive behavior [9,14,27,48,51]. As a result, it has been determined that the stable photocapacitance and photoconductance states can be changed according to the NiO:CdO ratio.

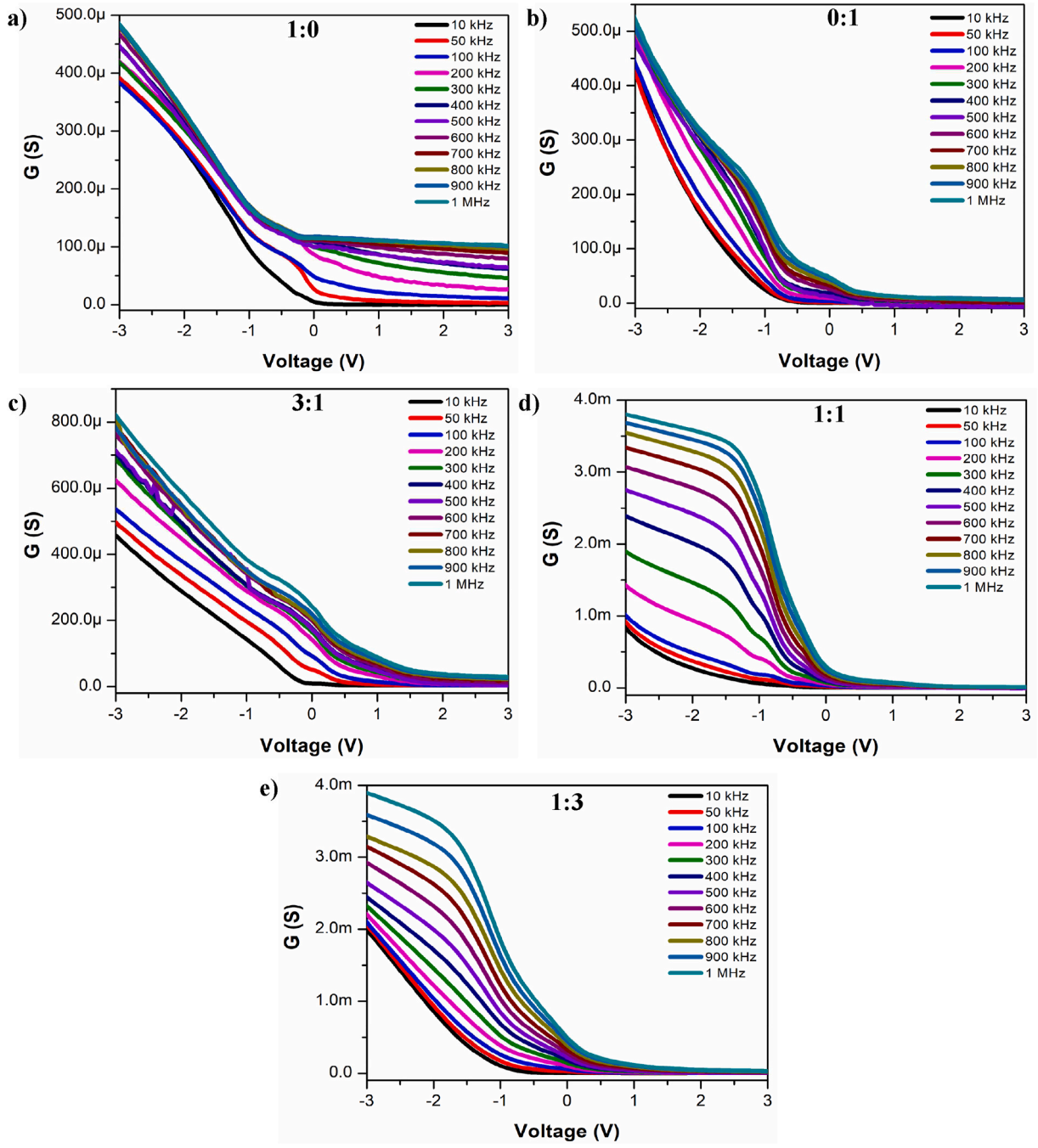

Fig. 13. The G-V characteristics of fabricated photodiodes at different NiO:CdO ratios a) 1:0, b) 0:1, c) 3:1, d) 1:1, and e) 1:3.

3.4. C–V and G-V characteristics of fabricated photodiodes

The C–V and G-V measurements of the fabricated Al/NiO:CdO/p-Si/Al photodiodes were performed to better characterize their electrical behavior. The C–V and G-V graphs at different frequencies (10 kHz–1 MHz) are shown in Fig. 12 and Fig. 13, respectively. In the reverse bias region of the NiO photodiode, a peak occurred at only 10 kHz frequency, and as the frequency increased, the peaks began to appear in the forward bias. In CdO and composite photodiodes, it was observed that the peaks occurred in the reverse bias region at all frequency values. The presence of these peaks can be explained by state changes at the interface, series resistance, and carriers captured in the case of band tails [47,51]. The positions of the peaks changed according to the NiO:CdO ratio, and as the frequency increased, the peaks were formed at lower voltage values in other photodiodes except NiO. The capacitance values decreased with increasing frequency in all circuit components. This is attributed to the presence of trapped charges in interface states that respond to signal variation and the response of charge carriers to AC signals at low frequency values [9,27,46,54]. As the NiO:CdO ratio changes, the number of interface charges can be changed and thereby the capacitance profile can be controlled [10]. The highest capacitance value was obtained in the composite photodiode with a 1:1 NiO:CdO ratio, and the capacitance values of the composite photodiodes were higher than those of pure ones. The capacitance of NiO:CdO/p-Si based photodiodes can be adjusted by changing the NiO:CdO ratio. The conductivity values were also affected by the frequency and voltage changes, and unlike the capacitance, the conductivity increased in all photodiodes as the frequency increased. This increase confirms the existence of interface state

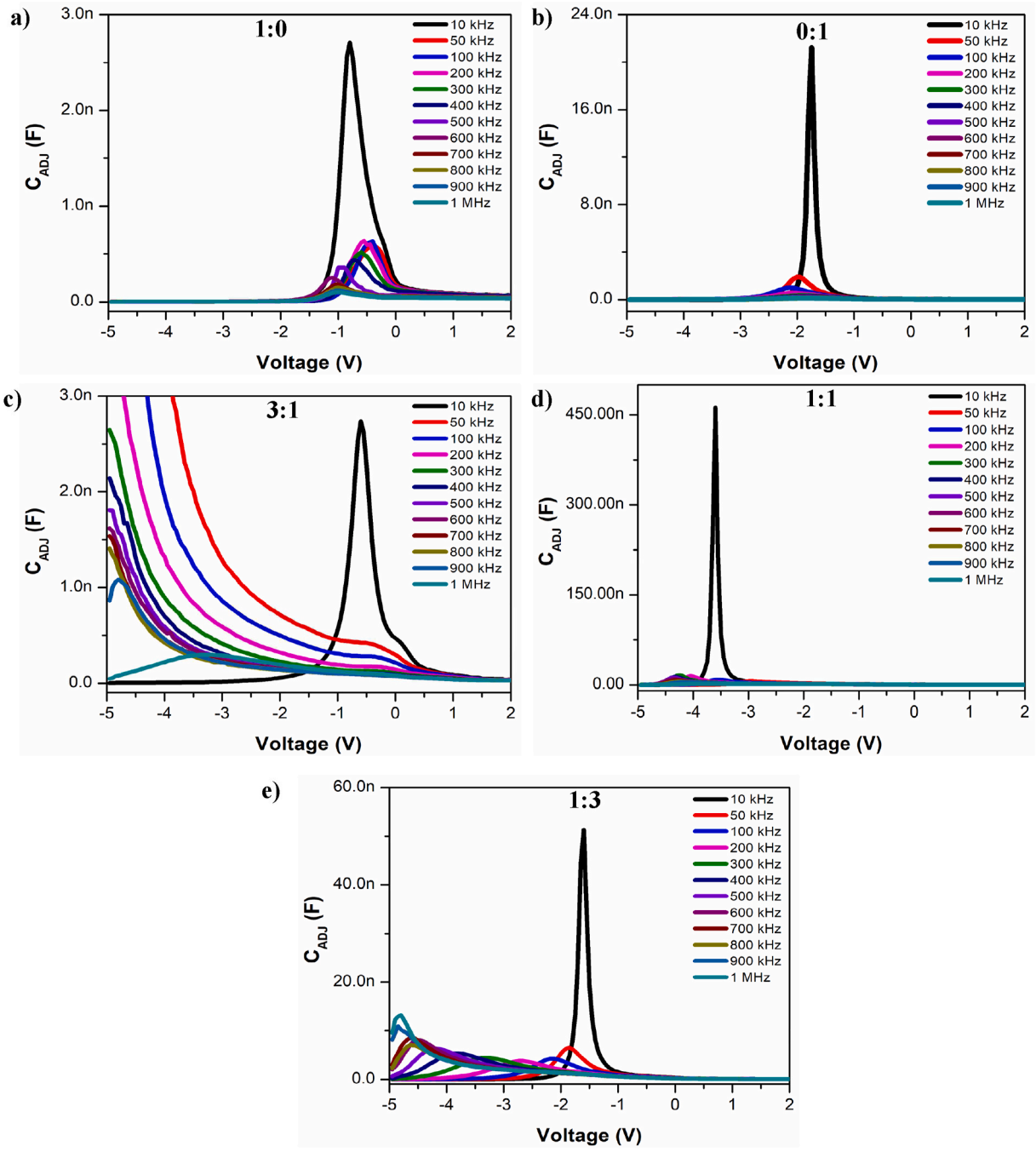

Fig. 14. The C_{ADJ}-V characteristics of fabricated photodiodes at different NiO:CdO ratios a) 1:0, b) 0:1, c) 3:1, d) 1:1, and e) 1:3.

[14,47,51]. The highest conductivity value was obtained in the composite photodiode with high CdO ratio and the conductivity values of the composite samples were higher than the pure ones. In addition, the conductivity value increased as the CdO ratio increased in composite photodiodes. In the study of ZnO:CdO composite photodiode in the literature, the photodiode with high CdO ratio provided the highest conductivity value [27]. From the C–V and G-V measurements, it has been seen that the capacitance and conductivity of the fabricated photodiodes are affected by the series resistance. This effect can theoretically be corrected or eliminated [9,27]. The capacitance and conductivity can be corrected with the help of the following equations [9,55,56];

$$C_{ADJ} = \frac{\left[G_m^2 + (\omega C_m)^2\right] C_m}{a^2 + (\omega C_m)^2} \tag{8}$$

$$G_{ADJ} = \frac{\left[G_m^2 + (\omega C_m)^2\right] a}{a^2 + (\omega C_m)^2} \tag{9}$$

where, C_{ADJ}, G_{ADJ}, C_m, G_m and ω denote corrected capacitance, corrected conductivity, measured capacitance, measured conductivity, and angular frequency, respectively. The a value in the equations can be calculated with the following equation [9,55,56];

$$a = G_m - \left[G_m^2 + (\omega C_m)^2\right] R_s \tag{10}$$

The C_{ADJ}-V and G_{ADJ}-V graphs of Al/NiO:CdO/p-Si/Al photodiodes

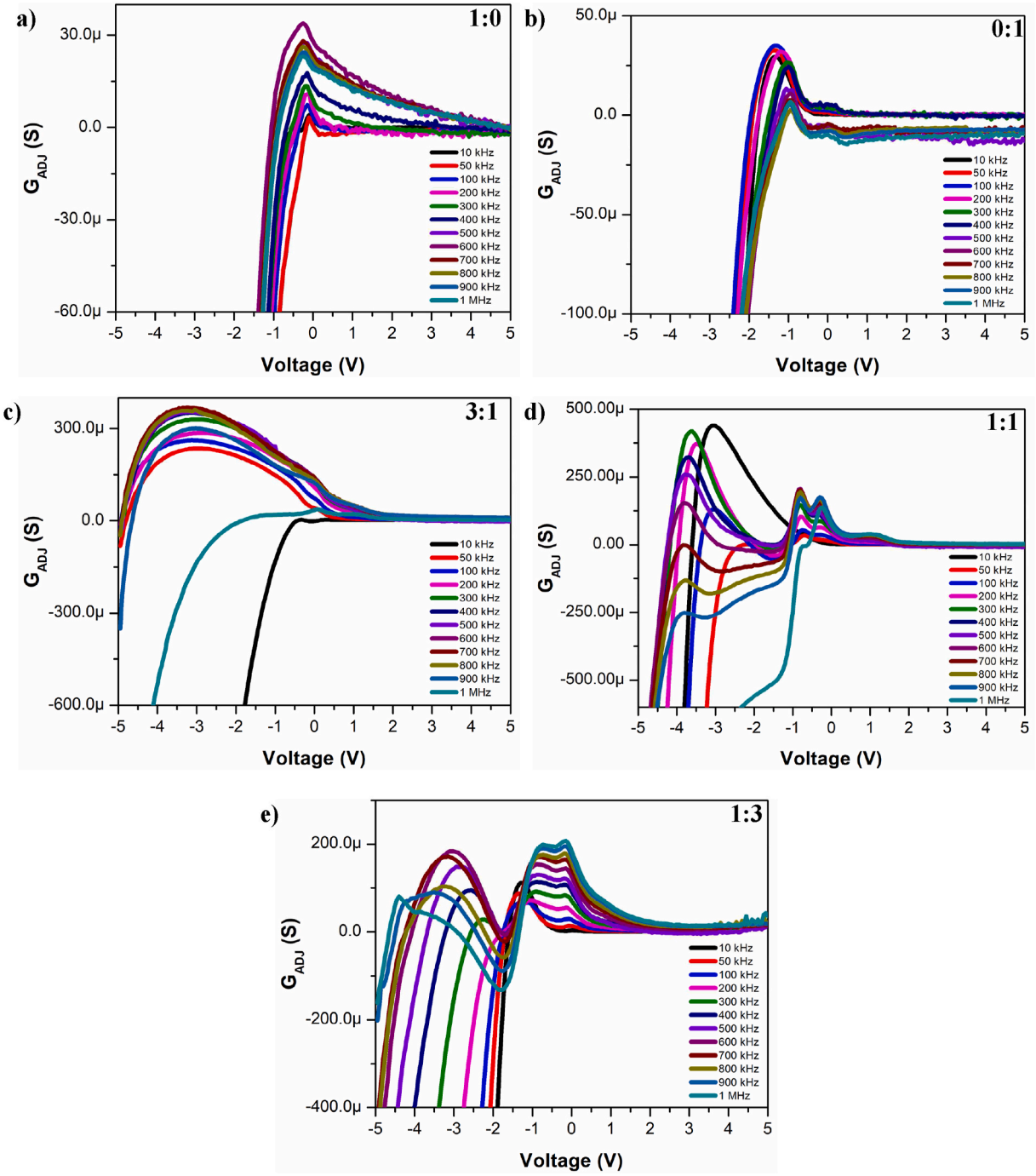

Fig. 15. The G_{ADJ}-V characteristics of fabricated photodiodes at different NiO:CdO ratios a) 1:0, b) 0:1, c) 3:1, d) 1:1, and e) 1:3.

with frequency values ranging from 10 kHz to 1 MHz are shown in Fig. 14 and Fig. 15, respectively. Peaks appeared in the negative bias region of the C_{ADJ}-V graphs and these peaks decreased at higher frequencies. In pure photodiodes, the peaks generally decreased as the frequency increased, whereas in composite samples, peaks of different intensity occurred depending on the frequencies. These peaks demonstrate the existence of series resistance and interface states [8,26,51]. In the forward bias region, the frequency and voltage changes did not affect the C_{ADJ}-V and remained constant during the time. In the G_{ADJ}-V graphs, peaks were formed in the negative bias regions, and the positions and intensities of these peaks changed as the NiO:CdO ratio changed. While there was a clear single peak in pure photodiodes, several peaks were observed in composite photodiodes. It can be inferred by the presence of series resistance and interface states [8,12,57]. The composite photodiodes have higher G_{ADJ} values than pure ones, and the photodiode with the highest G_{ADJ} value is the composite photodiode containing 1:1 NiO:CdO. It has been concluded that the C_{ADJ} and G_{ADJ} values of the photodiodes can be controlled and changed by changing the NiO:CdO ratio.

The capacitance and conductivity of photodiodes are significantly affected by the series resistance (R_S). For this reason, in order to better understand the non-linear behavior in the capacitance and conductivity of photodiodes, R_S characteristics of photodiodes should be known. The R_S values can be calculated with the following equation [9,58,59];

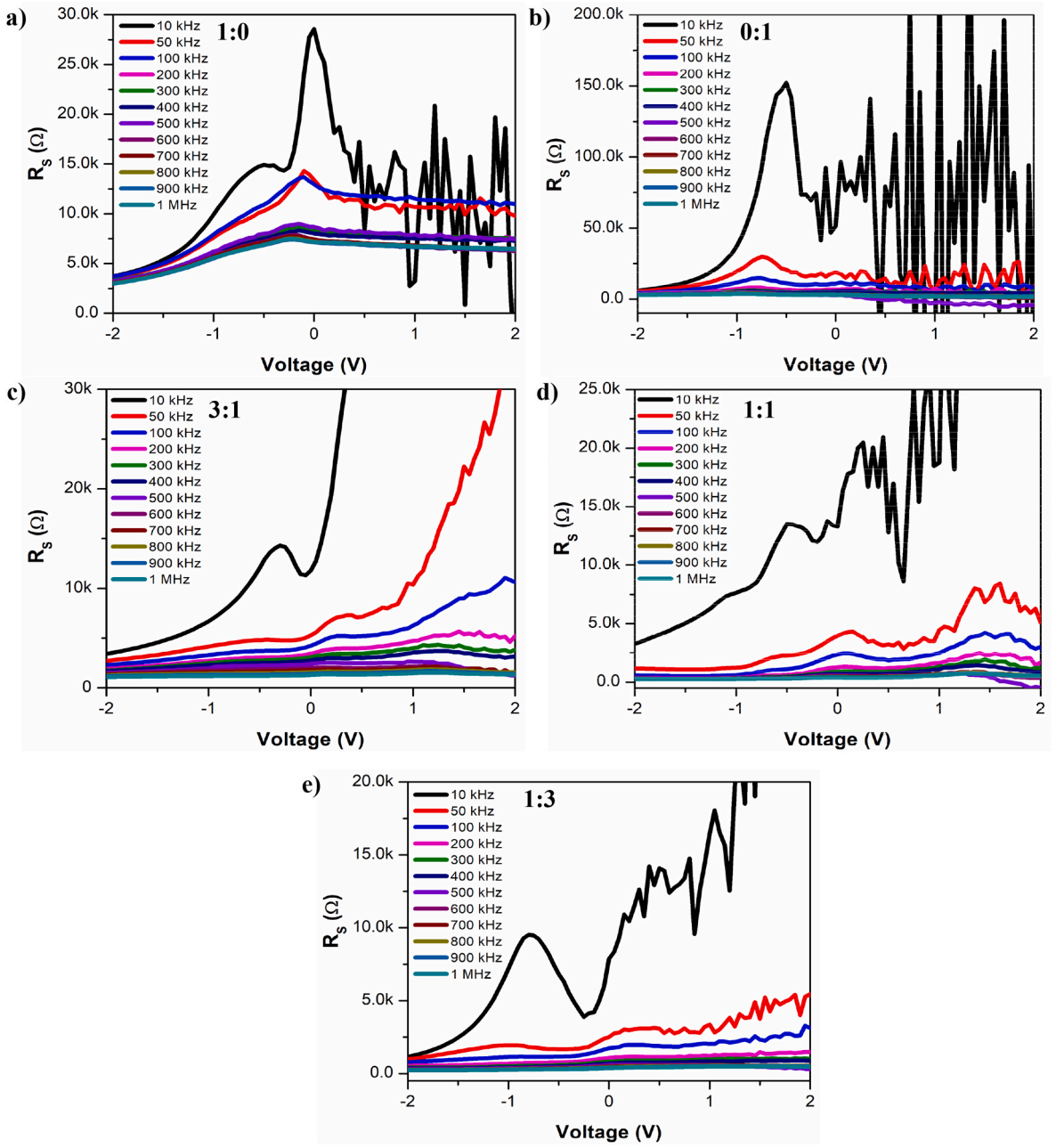

Fig. 16. The R_S-V characteristics of fabricated photodiodes at different NiO:CdO ratios a) 1:0, b) 0:1, c) 3:1, d) 1:1, and e) 1:3.

$$R_S = \frac{G_m}{G_m^2 + (\omega C_m)^2} \tag{11}$$

The voltage-dependent graphs of the R_S values of photodiodes at different frequency values (10 kHz–1 MHz) are seen in Fig. 16. As can be seen, peaks occurred in R_S values and these peaks decreased as the frequency increased. This is attributed the low frequencies followed by the interface states, and thus, more resistance has emerged at low frequency values [9]. In addition, the R_S values and the magnitudes of the peaks decreased as the frequency increased that resulted from the number of interface charge carriers and these carriers following the frequencies [9,18]. It should be noted that the changes in R_S values depending on the change in frequency occur due to different localized interface charges (trapped, fixed and mobile oxide charges) [47]. As the NiO:CdO ratio changed, different R_S values and R_S-V behaviors were observed. These results show that the R_S values of the photodiodes are affected by the frequency and the change in the NiO:CdO ratio. From these results, the important parameters of the photodiodes are significantly affected by the density of the interface states. Therefore, it is very important to determine the interface state densities (Dit) of photodiodes [9]. The following equation can be used to obtain the D_{it} values of a photodiode [9,60];

$$D_{it} = \frac{2}{qA} \frac{(G_{max}/\omega)}{\left[\left(\frac{G_{max}}{\omega C_{ox}}\right)^2 + \left(1 - \frac{C_m}{C_{ox}}\right)^2\right]} \tag{12}$$

Here, C_{ox} and G_{max} are the capacitance of the insulating layer and the measured maximum conductivity, respectively. In Fig. 17, the frequency-dependent changes of the D_{it} values of the photodiodes are shown. The D_{it} values of the photodiodes decreased due to the increase in frequency and became almost stable, especially at high frequencies. The decrease in the D_{it} values of the photodiodes due to the increase in frequency is attributed to the inability of the interface charge carriers to

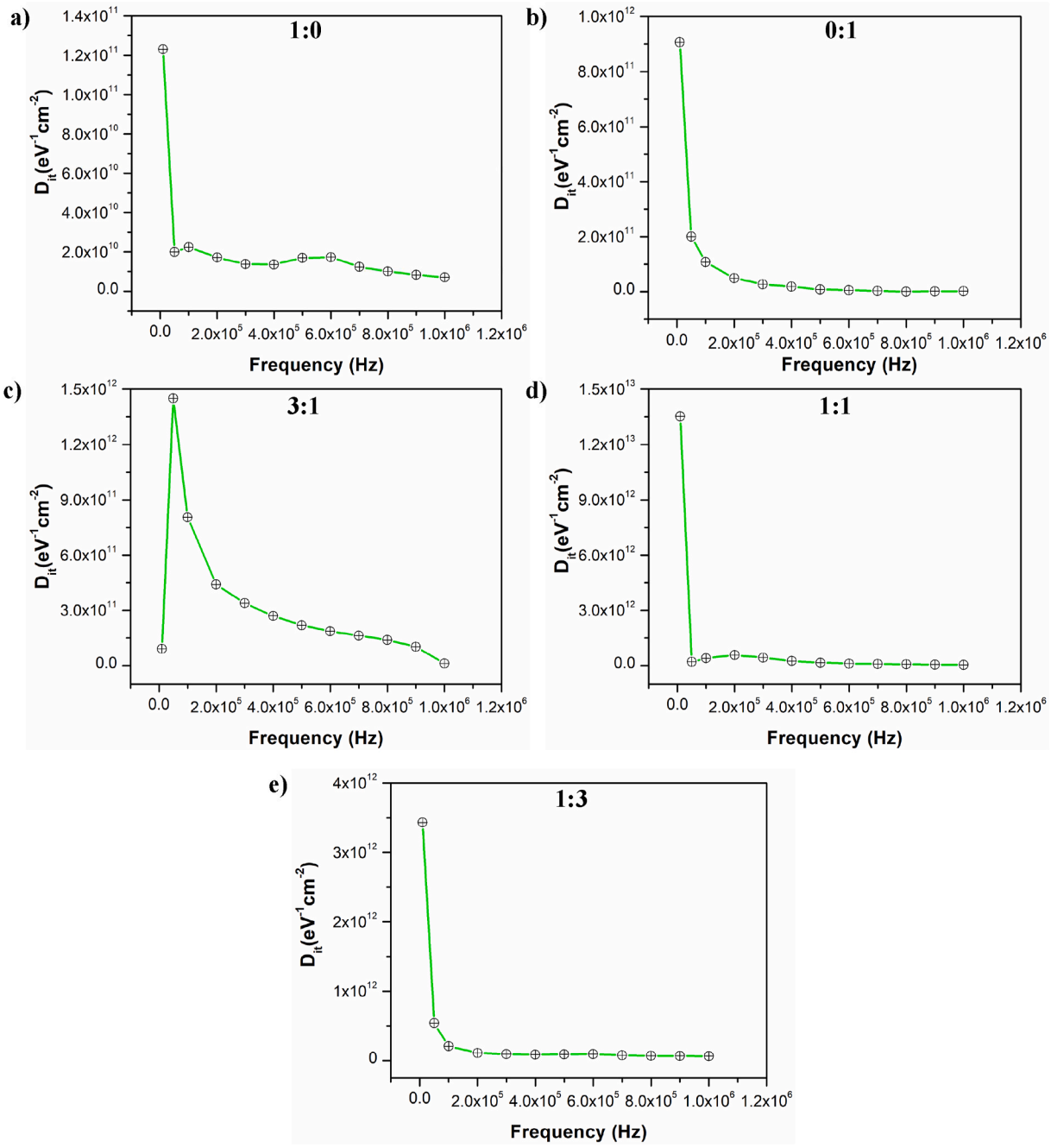

Fig. 17. Plots of D_{it} – F of fabricated photodiodes at different NiO:CdO ratios a) 1:0, b) 0:1, c) 3:1, d) 1:1, and e) 1:3.

follow the AC signal at high frequency values [26,61]. As the NiO:CdO ratio changed, different D_{it} values were obtained and the D_{it} values of the composite photodiodes were higher than those of pure ones, especially at low frequency values. At high frequency values, the D_{it} values of all fabricated photodiodes are very close to each other. These changes in the D_{it} values of the photodiodes are relevant to the occurrence of the interface states and the rearrangement of these interface states due to the change in the composition of the composite structures formed at the NiO:CdO interface [27]. From the D_{it}-V graphs, it is clear that the interface states are highly frequency dependent and the interface state densities can be changed by changing the NiO:CdO ratio.

4. Conclusions

The Al/NiO:CdO/p-Si/Al composite-based photodiodes were successfully fabricated by a dynamic sol-gel spin coating technique. The mineralogical analysis results of the composite thin films confirmed the peaks of NiO and CdO. Morphological analyses showed that the thin films were composed of nanostructures. The NiO coating consists of fine-grained aggregated nanoparticles, and the CdO coating consists of nano flower-like structures. The composite films consisted of quasi-spherical, non-uniform and stacked granule-like structures. The photoresponse, conductivity and capacitance properties of photodiodes were mainly controlled by light. Moreover, the photodiodes are sensitive to light and show rectification property. The highest photoresponse value was obtained in NiO photodiode. The all fabricated photodiodes have photoconductive and photocapacitance properties. The influence of voltage and frequency on the electrical properties of fabricated photodiodes was significant. The interface states have a remarkable significant effect on the parameters of the photodiodes. The photodiodes with different

properties could be obtained by changing the NiO:CdO ratio. Combining with these results, the fabricated Al/NiO:CdO/p-Si/Al composite photodiodes could find use area in the electronics industry and photosensitive optoelectronic applications.

Credit Author Statement

Ezgi Gürgenç: Conceptualization, Methodology, Visualization, Investigation, Writing – original draft preparation, Reviewing and Editing; Aydın Dikici: Supervision; Fehmi Aslan: Visualization, Investigation, preparation, Reviewing and Editing.

Declaration of competing interest

The authors declare that they have no known competing financial interests or personal relationships that could have appeared to influence the work reported in this paper.

Acknowledgements

The authors thank the Firat University Research Fund (FUBAP-TEKF.21.11) for their financial contribution to this research and the author Ezgi GURGENC would like to thank Council of Higher Education (CoHE) for its scholarship support with the 100/2000 Ph.D. scholarship.

References

[1] C.-K. Yang, T.-C. Cheng, C.-H. Cheng, C.-C. Wang, C.-C. Lee, Open-loop altitude-azimuth concentrated solar tracking system for solar-thermal applications, Sol. Energy 147 (2017) 52–60, https://doi.org/10.1016/j.solener.2017.03.014.
[2] W. Nsengiyumva, S.G. Chen, L. Hu, X. Chen, Recent advancements and challenges in solar tracking systems (STS): a review, Renew. Sustain. Energy Rev. 81 (2018) 250–279, https://doi.org/10.1016/j.rser.2017.06.085.
[3] S.S. Eldin, M. Abd-Elhady, H. Kandil, Feasibility of solar tracking systems for PV panels in hot and cold regions, Renew. Energy 85 (2016) 228–233, https://doi.org/10.1016/j.renene.2015.06.051.
[4] A. Hafez, A. Yousef, N. Harag, Solar tracking systems: technologies and trackers drive types–A review, Renew. Sustain. Energy Rev. 91 (2018) 754–782, https://doi.org/10.1016/j.rser.2018.03.094.
[5] M. Sidek, N. Azis, W. Hasan, M. Ab Kadir, S. Shafie, M. Radzi, Automated positioning dual-axis solar tracking system with precision elevation and azimuth angle control, Energy 124 (2017) 160–170, https://doi.org/10.1016/j.energy.2017.02.001.
[6] C.-P. Chen, P.-H. Lin, L.-Y. Chen, M.-Y. Ke, Y.-W. Cheng, J. Huang, Nanoparticle-coated n-ZnO/p-Si photodiodes with improved photoresponsivities and acceptance angles for potential solar cell applications, Nanotechnology 20 (2009) 245204, https://doi.org/10.1088/0957-4484/20/24/245204.
[7] F. Aslan, H. Esen, F. Yakuphanoglu, The effect of coumarin addition on the electrical characteristics of Al/Coumarin: CdO/p-Si/Al photodiode prepared by drop casting technique, Optik 197 (2019) 163203, https://doi.org/10.1016/j.ijleo.2019.163203.
[8] A. Tataroğlu, H. Aydın, A.A. Al-Ghamdi, F. El-Tantawy, W. Farooq, F. Yakuphanoglu, Photoconducting properties of Cd 0.4 ZnO 0.6/p-Si photodiode by sol gel method, J. Electroceram. 32 (2014) 369–375, https://doi.org/10.1007/s10832-014-9920-6.
[9] B.A. Gozeh, A. Karabulut, C.B. Ismael, S.I. Saleh, F. Yakuphanoglu, Zn-doped CdO effects on the optical, electrical and photoresponse properties of heterojunctions-based photodiodes, J. Alloys Compd. 872 (2021) 159624, https://doi.org/10.1016/j.jallcom.2021.159624.
[10] N. Khusayfan, Fabrication of the solar light sensitive ZnO1-xMgOx/n-Si photodiodes, J. Mol. Struct. 1224 (2021) 129030, https://doi.org/10.1016/j.molstruc.2020.129030.
[11] S. Demirezen, S.A. Yerişkin, A detailed comparative study on electrical and photovoltaic characteristics of Al/p-Si photodiodes with coumarin-doped PVA interfacial layer: the effect of doping concentration, Polym. Bull. 77 (2020) 49–71, https://doi.org/10.1007/s00289-019-02704-3.
[12] F. Yakuphanoglu, Transparent metal oxide films based sensors for solar tracking applications, Compos. B Eng. 92 (2016) 151–159, https://doi.org/10.1016/j.compositesb.2016.02.039.
[13] B.A.H. Ameen, A. Yildiz, W. Farooq, F. Yakuphanoglu, Solar light photodetectors based on nanocrystalline zinc oxide cadmium doped/p-Si heterojunctions, Silicon 11 (2019) 563–571, https://doi.org/10.1007/s12633-017-9656-4.
[14] N.M. Khusayfan, Electrical and photoresponse properties of Al/graphene oxide doped NiO nanocomposite/p-Si/Al photodiodes, J. Alloys Compd. 666 (2016) 501–506, https://doi.org/10.1016/j.jallcom.2016.01.102.
[15] M. Soylu, A. Dere, A.G. Al-Sehemi, A.A. Al-Ghamdi, F. Yakuphanoglu, Effect of calcination and carbon incorporation on NiO nanowires for photodiode performance, Microelectron. Eng. 202 (2018) 51–59, https://doi.org/10.1016/j.mee.2018.10.007.
[16] A. Farag, A. Mansour, A. Ammar, M.A. Rafea, A. Farid, Electrical conductivity, dielectric properties and optical absorption of organic based nanocrystalline sodium copper chlorophyllin for photodiode application, J. Alloys Compd. 513 (2012) 404–413, https://doi.org/10.1016/j.jallcom.2011.10.058.
[17] A.G. Al-Sehemi, K. Mensah-Darkwa, A.A. Al-Ghamdi, M. Soylu, R. Gupta, F. Yakuphanoglu, Composite CuFe1− xSnxO2/p-type silicon photodiodes, Spectrochim. Acta Mol. Biomol. Spectrosc. 180 (2017) 110–118, https://doi.org/10.1016/j.saa.2017.03.004.
[18] R. Gupta, A. Hendi, M. Cavas, A.A. Al-Ghamdi, O.A. Al-Hartomy, R. Aloraini, F. El-Tantawy, F. Yakuphanoglu, Improvement of photoresponse properties of NiO/p-Si photodiodes by copper dopant, Physica E Low Dimens. Syst. Nanostruct. 56 (2014) 288–295, https://doi.org/10.1016/j.physe.2013.09.014.
[19] A.M. El Nahrawy, A. Elzwawy, A.B. Abou Hammad, A. Mansour, Influence of NiO on structural, optical, and magnetic properties of Al2O3–P2O5–Na2O magnetic porous nanocomposites nucleated by SiO2, Solid State Sci. 108 (2020) 106454, https://doi.org/10.1016/j.solidstatesciences.2020.106454.
[20] A.M. El Nahrawy, B.A. Hemdan, A. Mansour, A. Elzwawy, A.B. AbouHammad, Structural and opto-magnetic properties of nickel magnesium copper zircon silicate nano-composite for suppress the spread of foodborne pathogenic bacteria, Silicon (2021) 1–16, https://doi.org/10.1007/s12633-021-01295-x.
[21] M. Rajini, S. Vinoth, K. Hariprasad, M. Karunakaran, K. Kasirajan, N. Chidhambaram, T. Ahamad, S.M. Alshehri, Tuning the optoelectronic properties of n-CdO: Fe/p-Si photodiodes fabricated by facile perfume atomizer technique for photo-detector applications, Appl. Phys. B 127 (2021) 1–11, https://doi.org/10.1007/s00340-021-07658-x.
[22] K. Kasirajan, A.N.A. Anasthasiya, O.M. Aldossary, M. Ubaidullah, M. Karunakaran, Structural, morphological, optical and enhanced photodetection activities of CdO films: an effect of Mn doping, Sens. Actuator A Phys. 319 (2021) 112531, https://doi.org/10.1016/j.sna.2020.112531.
[23] I.L.P. Raj, N. Chidhambaram, S. Saravanakumar, S. Sasikumar, S. Varadharajaperumal, D. Alagarasan, T. Alshahrani, M. Shkir, S. AlFaify, A comprehensive study on effect of annealing on structural, morphological and optical properties of CdO and photodetection of heterojunction n-CdO/p-Si diode, Optik 241 (2021) 166406, https://doi.org/10.1016/j.ijleo.2021.166406.
[24] A.M. Afzal, I.-G. Bae, Y. Aggarwal, J. Park, H.-R. Jeong, E.H. Choi, B. Park, Highly efficient self-powered perovskite photodiode with an electron-blocking hole-transport NiO x layer, Sci. Rep. 11 (2021) 1–14, https://doi.org/10.1038/s41598-020-80640-3.
[25] F.E. Al-Hazmi, F. Yakuphanoglu, Photoconducting and photovoltaic properties of ZnO:TiO2 composite/p-silicon heterojunction photodiode, Silicon 10 (2018) 781–787, https://doi.org/10.1007/s12633-016-9530-9.
[26] A. Karabulut, A. Dere, A.G. Al-Sehemi, A.A. Al-Ghamdi, F. Yakuphanoglu, Cadmium oxide: titanium dioxide composite based photosensitive diode, J. Electron. Mater. 47 (2018) 7159–7169, https://doi.org/10.1007/s11664-018-6647-1.
[27] A. Sevik, B. Coskun, M. Soylu, The effect of molar ratio on the photo-generated charge activity of ZnO–CdO composites, Eur. Phys. J. Plus. 135 (2020) 65, https://doi.org/10.1140/epjp/s13360-020-00129-w.
[28] J.-D. Hwang, W.-M. Lin, Enhancing the photoresponse of p-NiO/n-ZnO heterojunction photodiodes using post ZnO treatment, IEEE Trans. Nanotechnol. 18 (2018) 126–131, https://doi.org/10.1109/TNANO.2018.2884936.
[29] N. Park, K. Sun, Z. Sun, Y. Jing, D. Wang, High efficiency NiO/ZnO heterojunction UV photodiode by sol–gel processing, J. Mater. Chem. C. 1 (2013) 7333–7338, https://doi.org/10.1039/C3TC31444H.
[30] A. Al-Ghamdi, W.E. Mahmoud, S.J. Yaghmour, F. Al-Marzouki, Structure and optical properties of nanocrystalline NiO thin film synthesized by sol–gel spin-coating method, J. Alloys Compd. 486 (2009) 9–13, https://doi.org/10.1016/j.jallcom.2009.06.139.
[31] S. Zhao, Y. Shen, P. Zhou, J. Zhang, W. Zhang, X. Chen, D. Wei, P. Fang, Y. Shen, Highly selective NO2 sensor based on p-type nanocrystalline NiO thin films prepared by sol–gel dip coating, Ceram. Int. 44 (2018) 753–759, https://doi.org/10.1016/j.ceramint.2017.09.243.
[32] R. Zargar, S. Chackrabarti, M. Malik, A. Hafiz, Sol-gel syringe spray coating: a novel approach for Rietveld, optical and electrical analysis of CdO Film for optoelectronic applications, Phys. Open. 7 (2021) 100069, https://doi.org/10.1016/j.physo.2021.100069.
[33] R. Kumari, V. Kumar, Impact of zinc doping on structural, optical, and electrical properties of CdO films prepared by sol–gel screen printing mechanism, J. Sol. Gel Sci. Technol. 94 (2020) 648–657, https://doi.org/10.1007/s10971-019-05202-0.
[34] H. Karimi-Maleh, A.L. Sanati, V.K. Gupta, M. Yoosefian, M. Asif, A. Bahari, A voltammetric biosensor based on ionic liquid/NiO nanoparticle modified carbon paste electrode for the determination of nicotinamide adenine dinucleotide (NADH), Sensor. Actuator. B Chem. 204 (2014) 647–654, https://doi.org/10.1016/j.snb.2014.08.037.
[35] J.K. Rajput, T.K. Pathak, V. Kumar, M. Kumar, L. Purohit, Annealing temperature dependent investigations on nano-cauliflower like structure of CdO thin film grown by sol–gel method, Surface. Interfac. 6 (2017) 11–17, https://doi.org/10.1016/j.surfin.2016.11.005.
[36] V. Ganesh, S. AlFaify, Linear and nonlinear optical properties of sol-gel spin coated erbium-doped CdO thin films, Phys. B Condens. Matter 570 (2019) 58–65, https://doi.org/10.1016/j.physb.2019.05.045.
[37] E.F.A. Zeid, I.A. Ibrahem, A.M. Ali, W.A. Mohamed, The effect of CdO content on the crystal structure, surface morphology, optical properties and photocatalytic

efficiency of p-NiO/n-CdO nanocomposite, Results Phys. 12 (2019) 562–570, https://doi.org/10.1016/j.rinp.2018.12.009.
[38] S. Anitha, M. Suganya, D. Prabha, J. Srivind, S. Balamurugan, A. Balu, Synthesis and characterization of NiO-CdO composite materials towards photoconductive and antibacterial applications, Mater. Chem. Phys. 211 (2018) 88–96, https://doi.org/10.1016/j.matchemphys.2018.01.048.
[39] X.L. Wang, Z. Liu, C. Wen, Y. Liu, H.Z. Wang, T. Chen, H.Y. Zhang, Thickness effect of nickel oxide thin films on associated solution-processed write-once-read-many-times memory devices, Appl. Phys. A 124 (2018) 1–7, https://doi.org/10.1007/s00339-018-1868-y.
[40] J. Wang, P. Yang, X. Wei, Z. Zhou, Preparation of NiO two-dimensional grainy films and their high-performance gas sensors for ammonia detection, Nanoscale Res. Lett. 10 (2015) 1–6, https://doi.org/10.1186/s11671-015-0807-5.
[41] S.T. Akinkuade, W.E. Meyer, J.M. Nel, Effects of thermal treatment on structural, optical and electrical properties of NiO thin films, Phys. B Condens. Matter 575 (2019) 411694, https://doi.org/10.1016/j.physb.2019.411694.
[42] J.K. Rajput, T.K. Pathak, H.C. Swart, L.P. Purohit, Synthesis of CdO nanoflowers by Sol-Gel method on different substrates with photodetection application, Phys. Status Solidi 216 (2019) 1900093, https://doi.org/10.1002/pssa.201900093.
[43] Y.S. Ocak, D. Batibay, S. Baturay, Optical and electrical properties of Ni-doped CdO thin films by ultrasonic spray pyrolysis, J. Mater. Sci. Mater. Electron. 29 (2018) 17425–17431, https://doi.org/10.1007/s10854-018-9841-2.
[44] I.B. Miled, M. Jlassi, I. Sta, M. Dhaouadi, M. Hajji, G. Mousdis, M. Kompitsas, H. Ezzaouia, Influence of In-doping on microstructure, optical and electrical properties of sol–gel derived CdO thin films, J. Mater. Sci. Mater. Electron. 29 (2018) 11286–11295, https://doi.org/10.1007/s10854-018-9216-8.
[45] A. Wassilkowska, A. Czaplicka-Kotas, A. Bielski, M. Zielina, An analysis of the elemental composition of micro-samples using EDS technique, Tech. Trans. Chemia Zeszyt (18) (2014) 133–148, https://doi.org/10.4467/2353737XCT.14.283.3371, 1-Ch.
[46] S. Dugan, M.M. Koç, B. Coşkun, Structural, electrical and optical characterization of Mn doped CdO photodiodes, J. Mol. Struct. 1202 (2020) 127235, https://doi.org/10.1016/j.molstruc.2019.127235.
[47] S.A. Pehlivanoglu, Fabrication of p-Si/n-NiO: Zn photodiodes and current/capacitance-voltage characterizations, Phys. B Condens. Matter 603 (2021) 412482, https://doi.org/10.1016/j.physb.2020.412482.
[48] F. Aslan, H. Esen, F. Yakuphanoglu, Al/P-Si/Coumarin: TiO2/Al organic-inorganic hybrid photodiodes: investigation of electrical and structural properties, Silicon 12 (2020) 2149–2164, https://doi.org/10.1007/s12633-019-00306-2.
[49] I. Zedan, E. El-Menyawy, A. Mansour, Physical characterizations of 3-(4-methyl piperazinylimino methyl) rifampicin films for photodiode applications, Silicon 11 (2019) 1693–1699, https://doi.org/10.1007/s12633-018-9989-7.
[50] A. Mansour, A.B. Abou Hammad, A.M. El Nahrawy, Sol–gel synthesis and physical characterization of novel MgCrO4-MgCu2O3 layered films and MgCrO4-MgCu2O3/p-Si based photodiode, Nano-Struct. Nano-Objects 25 (2021) 100646, https://doi.org/10.1016/j.nanoso.2020.100646.
[51] F. Aslan, H. Esen, F. Yakuphanoglu, Electrical and fotoconducting characterization of Al/coumarin: ZnO/Al novel organic-inorganic hybrid photodiodes, J. Alloys Compd. 789 (2019) 595–606, https://doi.org/10.1016/j.jallcom.2019.03.090.
[52] A. Mansour, Fabrication and characterization of a photodiode based on 5′, 5′′-dibromo-o-cresolsulfophthalein (BCP), Silicon 11 (2019) 1989–1996, https://doi.org/10.1007/s12633-018-0016-9.
[53] N.A. Elkanzi, A. Farag, N. Roushdy, A. Mansour, Design, fabrication and optical characterizations of pyrimidine fused quinolone carboxylate moiety for photodiode applications, Optik 216 (2020) 164882, https://doi.org/10.1016/j.ijleo.2020.164882.
[54] A. Farag, W. Osiris, A. Ammar, A. Mansour, Electrical and photosensing performance of heterojunction device based on organic thin film structure, Synth. Met. 175 (2013) 81–87, https://doi.org/10.1016/j.synthmet.2013.04.030.
[55] E. Nicollian, A. Goetzberger, The si-sio, interface–electrical properties as determined by the metal-insulator-silicon conductance technique, Bell Syst. Tech. J. 46 (1967), https://doi.org/10.1002/j.1538-7305.1967.tb01727.x, 1055-1033.
[56] E.H. Nicollian, J.R. Brews, E.H. Nicollian, MOS (Metal Oxide Semiconductor) Physics and Technology, Wiley, New York, 1982.
[57] A. Dere, M. Soylu, F. Yakuphanoglu, Solar light sensitive photodiode produced using a coumarin doped bismuth oxide composite, Mater. Sci. Semicond. Process. 90 (2019) 129–142, https://doi.org/10.1016/j.mssp.2018.10.009.
[58] İ. Dökme, Ş. Altındal, T. Tunç, İ. Uslu, Temperature dependent electrical and dielectric properties of Au/polyvinyl alcohol (Ni, Zn-doped)/n-Si Schottky diodes, Microelectron. Reliab. 50 (2010) 39–44, https://doi.org/10.1016/j.microrel.2009.09.005.
[59] E. Nicollian, A. Goetzberger, MOS conductance technique for measuring surface state parameters, Appl. Phys. Lett. 7 (1965) 216–219, https://doi.org/10.1063/1.1754385.
[60] W. Hill, C. Coleman, Solid-State Electron, JJ 491 (1980) 496.
[61] A.G. Imer, A. Dere, A.G. Al-Sehemi, O. Dayan, Z. Serbetci, A.A. Al-Ghamdi, F. Yakuphanoglu, Photosensing properties of ruthenium (II) complex-based photodiode, Appl. Phys. A 125 (2019) 1–10, https://doi.org/10.1007/s00339-019-2504-1.